Narrowband Violet Light-Emitting Diodes Based on Stable Cesium Lead Chloride Perovskite Nanocrystals

Congyang Zhang,[†] *Qun Wan,*[‡] *Luis K. Ono,*[†] *Yuqiang Liu,*[†] *Weilin Zheng,*[‡] *Qinggang Zhang,*[‡] *Mingming Liu,*[‡] *Long Kong,*[‡] *Liang Li,*[*,‡] *and Yabing Qi* [*,†]

[†]Energy Materials and Surface Sciences Unit (EMSSU), Okinawa Institute of Science and Technology Graduate University (OIST), 1919-1 Tancha, Onna-son, Kunigami-gun, Okinawa 904-0495, Japan.

[‡]School of Environmental Science and Engineering, Shanghai Jiao Tong University, 800 Dongchuan Road, Shanghai 200240, P.R. China.

***Corresponding Authors:**

Yabing Qi, Email: Yabing.Qi@OIST.jp; Liang Li, Email: liangli117@sjtu.edu.cn.

ABSTRACT

$CsPbCl_3$ nanocrystals are potential ultrapure emitters. But it is challenging to synthesize $CsPbCl_3$ nanocrystals with sufficient stability, which impedes their application in light-emitting devices. In this work, we report a facile phosphoryl chemistry mediated synthesis approach to synthesizing stable $CsPbCl_3$ nanocrystals, in which the phenylphosphonic dichloride ($PhPOCl_2$) precursor is employed. In addition to the high reactivity of the P-Cl bond of $PhPOCl_2$ for providing adequate Cl, the derived P=O with good proton affinity facilitates the formation of a distinct nanocrystal surface with the non-protonated oleylamine (OLA) ligand. Accordingly, the L-type ligand capped $CsPbCl_3$ nanocrystals exhibited not only bright luminance but also good stability that endures repeated purification up to 10 cycles. Based on the stable $CsPbCl_3$ nanocrystals, we achieved violet LEDs with extremely narrow electroluminescence spectra (full width at half-maximum ~ 10.6 nm).

TOC GRAPHICS

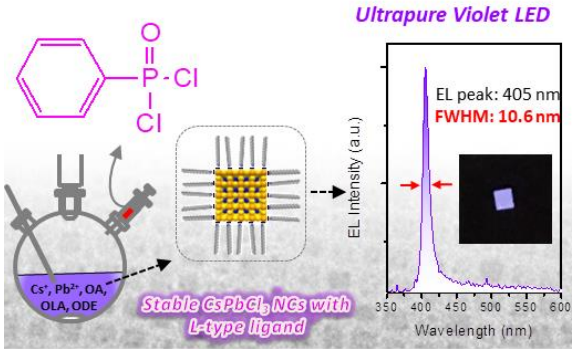

Exploitation and development of wide-bandgap semiconductor materials for short wavelength light-emitting diode (LED) have been a time-enduring research theme owing to their rich technological applications.[1] Despite many efforts, the studies on violet-emitting (< 435 nm) materials and LEDs are still very scarce, which yet are of great significance for a wide range of photonic and optoelectronic technologies, spanning from wide-gamut full-color displays, phototherapy, sensors, lasers, to optical detectors.[2-5] In this regard, LEDs based on group III nitrides (GaN, InGaN) and metal oxide (ZnO, SnO_2) still rendered the dominant violet emitting technology. But fabrication of these devices requires complex high-temperature and high-vacuum thin film deposition techniques.[6-8] Alternatively, thin-film LEDs based on organic semiconductors and quantum dots (QDs) provide unique opportunities for violet emission as well.[9-10] However, as shown in **Table 1**, owing to the material-related challenges, most of the demonstrated violet LEDs show broad electroluminescence (EL) linewidth, leading to significant energy loss. For instance, to reduce the emission linewidth and improve the color purity of broad emission in materials, color filters or optical microcavities are essential for the wide-gamut display application. It results in waste of emission energy and has a significant adverse effect on the device performance. Even for the colloidal QDs and nanoplatelets (NPLs) featuring narrow band-edge emission, the colloidal synthesis becomes challenging when violet emission with a large bandgap is required. The major technological hurdle is the difficulty to achieve highly confined, ultrasmall QDs/ultrathin NPLs without sophisticated shell coating processes.[17-18] Therefore, despite the challenges, it is still desirable to explore available simpler narrow violet-emitting materials, and it is of great significance to achieve such short wavelength LEDs with inexpensive and easier processing protocols.

Table 1. Comparison of our LED device with the reported blue/violet/ultraviolet LEDs.

Emitting Materials & Examples		EL Region (nm)	Fabrication Technology	EL FWHM (nm)	Ref
Group III Nitrides	GaN, InGaN	380-450	Metal organic chemical vapor deposition (MOCVD) or metal organic vapor phase epitaxy (MOVPE)	20-30	11
Metal Oxides	ZnO, SnO_2	390-410	MOCVD, MOVPE, Electrodeposition or Laser pulse deposition, etc.	20-80	7-8
Organic solid	Bi(9,9-diaryfluorene)s	380-450	Vacuum-based deposition (VBD)	>40	2, 9, 12-13
Chalcogenide QDs	Chalcogenide QDs (*e. g.* ZnCdS)	375-460	Solution-process	20-40	10, 14
C-Dots	C-Dots	425-475	Solution-process	>30	15
Perovskite film	$CsPb(Br_xCl_{1-x})_3$, Quasi-2D perovskite	465-490	Solution-process	15-50	16-17
Perovskite NCs	$CsPb(Br_xCl_{1-x})_3$ NCs, $Cs_3Sb_2Br_9$, Perovskite NPLs	410-470	Solution-process	12-30	18-22
	$CsPbCl_3$ NCs	405	Solution-process	**10.6**	**This work**

Recently, metal halide perovskite ($APbX_3$, A is a monovalent cation (*e. g.*, Cs^+, $CH_3NH_3^+$ (MA), or $CH(NH_2)_2^+$ (FA)), X is a halide anion (Cl, Br, or I)) have been envisioned as promising candidates for next generation light emitting applications.[23] Owing to the unique antibonding orbitals of the $[PbX_6]^{4-}$ octahedral determined band-edge state, metal halide perovskites feature tunable bandgap and emission wavelength (from near-infrared to violet) through composition engineering.[24] In addition, due to the crystal structure dependent electronic band and the unique defect tolerance, both perovskite polycrystalline films and nanocrystals (NCs) exhibit relatively high PLQY and narrow emission linewidth. As a result, significant breakthroughs of perovskite LEDs (PeLEDs) have been achieved during the past decade. Up to now, the highly efficient

green/red/near-infrared PeLEDs were demonstrated with Br- or I-based perovskites through a quasi-2D structure,[25-26] rational light extraction,[27-28] molecular passivation[29-32] and triplet management[33] strategies and so on. Recently, efficient blue perovskite emitters and LEDs have been developed as well. For instance, based on a bipolar-shell resurfacing strategy, Dong et al. reported highly confined $CsPbBr_3$ QDs with an PLQY of 90%, which led to the efficient blue PeLED with an record high EQE of 12.3%.[34] However, compared to the well-explored Br- and I-based perovskite, the development of the Cl-based violet emitting perovskite and LEDs still lags far behind, which yet shows a great potential for the ultrapure violet emission. Considering the thin-film fabrication difficulties of the Cl-based perovskites due to the low solubility of Cl-based precursors,[35] the colloidal route toward Cl-perovskite NCs has gained immense scientific interest. Actually, PLQY as high as near-unity and the full width at half maximum (FWHM) as low as 12 nm have been reported for the violet emitted $CsPbCl_3$ NCs.[36] As a result, the Cl-based perovskite NCs (such as $CsPbCl_3$) are the ideal emitter for fabricating efficient ultrapure violet LEDs.

The commonly used "two-precursor" hot-injection method was often employed for the synthesis of $CsPbCl_3$ NCs.[37] However, owing to the fixed low element ratios of halide to metal, the as-synthesized $CsPbCl_3$ NCs suffer from inferior PL emission with abundant trap states (Cl vacancies).[38-39] In view of this issue, Imran and co-workers developed a "three-precursor" synthesis approach for $CsPbCl_3$ NCs by using excess benzoyl chloride (PhCOCl) as the independent halide precursor. The as-synthesized $CsPbCl_3$ NCs exhibited enhanced PL (PLQY up to 65%).[40] Dutta et al. further employed the oleylammonium chloride (OLACl) as a dual precursor providing halide ions and the capping agent, thus facilitating the synthesis of desired $CsPbCl_3$ NCs with a near unity PLQY.[36] Besides, strategies based on *in situ* doping and post-

synthesis treatment of metal chloride salts are also proven to be highly effective in obtaining brightly luminescent $CsPbCl_3$ NCs.[38-39, 41-43]

However, despite the success of achieving high PLQY of $CsPbCl_3$ NCs, the $CsPbCl_3$ NCs based LEDs have not been demonstrated so far, which lag far behind the Br and I based ones. The major obstacle is originated from the poor stability of $CsPbCl_3$ NCs that can be further ascribed to the ligand related surface ion loss and abundant defect states. The excellent optical properties of $CsPbCl_3$ NCs are temporary and sensitive to purification and storage conditions.[43] Herein, we report a phosphoryl chemistry mediated synthesis approach to achieving highly luminescent and unprecedentedly stable $CsPbCl_3$ NCs. This new approach relies on the use of the phenylphosphonic dichloride ($PhPOCl_2$) as the alternative Cl source in the typical "three-precursor" hot-injection method. The direct injection of highly reactive $PhPOCl_2$ results in rapid nucleation and growth of $CsPbCl_3$ NCs delivering both excellent PL and robust stability, which is much better than the reported $CsPbCl_3$ NCs. It is remarkable that the bright violet emission can be maintained even after 10 cycles of purification. The detailed study of surface chemistry enabled identification that the greatly improved quality of $CsPbCl_3$ NCs can be mainly attributed to the distinctly reconstructed surface that is terminated with a $PbCl_x$-rich shell and capped with the non-protonated L-type ligand (Oleylamine, OLA) with strong binding ability. This can be further ascribed to the good protonation effect of derived P=O of the used $PhPOCl_2$ precursor. Finally, for the first time, employing the high-quality $CsPbCl_3$ NCs as the emitting layer, the solution-processed violet (405 nm) LED was demonstrated with extremely narrow EL spectra (FWHM = 10.6 nm), which is superior to almost all the reported LEDs with similar wavelengths.

In our synthesis approach of $CsPbCl_3$ NCs, $PhPOCl_2$ is employed as the efficient Cl precursor. $PhPOCl_2$ is a commonly used organic cross-linking agent for the condensation

reaction toward phosphorus-containing polymer or oligomer, in which the reactive P-Cl bonds can interact with nucleophilic compounds (such as amines, alcohols, carboxylic acids) and release HCl.[44-45] Compared with PhCOCl, a previously reported analogous Cl precursor,[40] $PhPOCl_2$ exhibits more negative reaction energy (-0.35 eV *vs.* -0.34 eV) and much lower kinetic barrier (1.43 eV *vs.* 3.95 eV) when reacted with a proton.[46] These calculation results clearly showed that $PhPOCl_2$ should be more reactive and prone to release HCl. This point was further verified by using PhCOCl and $PhPOCl_2$ as the anion exchange reagents for the pre-synthesized $CsPbBr_3$ NCs. As shown in **Figure S1**, both PhCOCl and $PhPOCl_2$ can effectively trigger halide exchange (from Br to Cl) of $CsPbBr_3$ NCs at room temperature, leading to the continuous blue-shift of the PL spectra. In contrast, $PhPOCl_2$ can drive the halide exchange with obviously faster reaction kinetics. In light of the vulnerable $CsPbCl_3$ NCs with easily formed Cl vacancy defects, a Cl-rich reaction environment is highly desirable. Therefore, $PhPOCl_2$ with stronger reactivity would be a better independent Cl source to provide more available Cl for the synthesis of $CsPbCl_3$ NCs. Furthermore, $PhPOCl_2$ is commercially avalaible and has a much higher boiling point (up to 260 °C), thus allowing us to synthesize at sufficiently high temperatures to get high-quality NCs with good reproducibility.

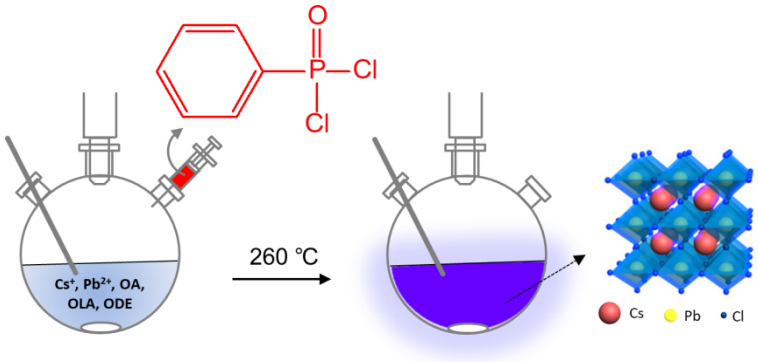

Scheme 1. Schematic diagram to illustrate the colloidal synthesis process of $CsPbCl_3$ NCs using $PhPOCl_2$ as the Cl precursor.

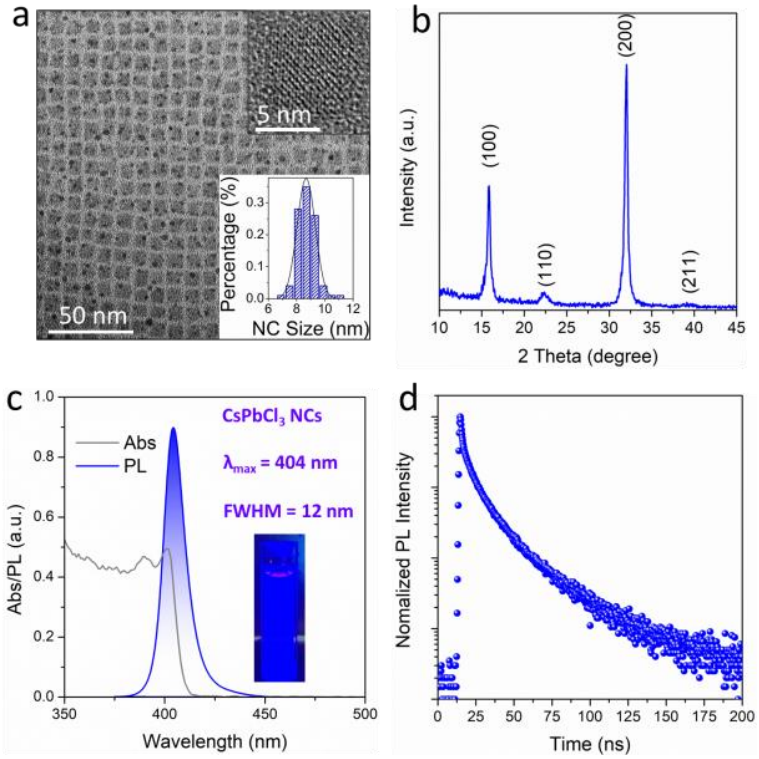

Figure 1. (a) TEM image (inset: corresponding high-resolution TEM image and size distribution), (b) XRD pattern, (c) Optical absorption and PL spectra (excitation wavelength 350 nm) (inset: corresponding photograph under UV light), and (d) time-resolved photoluminescence (TRPL) decay curve of the synthesized $PhPOCl_2$ based $CsPbCl_3$ NCs.

In a typical synthesis (**Scheme 1**, see **Experimental Section** for details), the Pb and Cs precursors were prepared in octadecene (ODE) with the assistance of oleic acid (OA) and OLA under dry argon gas. At 260 ℃, excess $PhPOCl_2$ was injected swiftly, and the colorless metal precursor solution turned white and turbid immediately, indicating the formation of $CsPbCl_3$ NCs. After 20 s, the reaction was quenched in ice bath and cooled to room temperature. The NCs were purified by centrifugation, and then re-dispersed in toluene. As indicated from the TEM

analysis **(Figure 1a and Figure S2)**, the as-synthesized product consisted of highly monodisperse cubic-shaped NCs with an average size of 8.8 nm (with the standard deviation of 0.4 nm). The lattice fringes can be clearly identified from the representative high-resolution TEM image (inset in **Figure 1a**). The crystal structure of the $CsPbCl_3$ NCs was confirmed by X-ray diffraction (XRD), which matches well with the cubic crystalline perovskite structure (**Figure 1b**). To study the optical property, the representative absorption and PL spectra were recorded. As shown in **Figure 1c,** the as-synthesized $CsPbCl_3$ NCs exhibit a sharp excitonic absorption peak at 402 nm and a narrow PL emission band centered at 404 nm (FWHM = 12 nm). The relatively small Stokes shift of ~15 meV suggested that the emission photons exclusively stem from the direct exciton recombination. The absolute PLQY of the as-synthesized $CsPbCl_3$ NCs in the diluted solution was measured using a fluorescence spectrometer coupled with an integrated sphere excited at a wavelength of 365 nm. A high value of 71% was obtained, which is much higher than most reported $CsPbCl_3$ NCs without post-modification. To gain more insight into exciton recombination dynamics, time-resolved PL was measured (**Figure 1d**). The PL decay of $CsPbCl_3$ NCs gives rise to a shorter lifetime component of 1.12 ns with a contribution of 91% and a longer lifetime component of 10.85 ns with a contribution of 9%, suggesting the predominant single recombination pathway. Therefore, this result further highlights the excellent optical property of as-synthesized $CsPbCl_3$ NCs. The high-quality $CsPbCl_3$ NCs obtained from $PhPOCl_2$ based approach can be further verified through direct comparison with the NCs synthesized from other reported Cl precursors.[36] **(see detail in Figure S3 and Figure S4)**

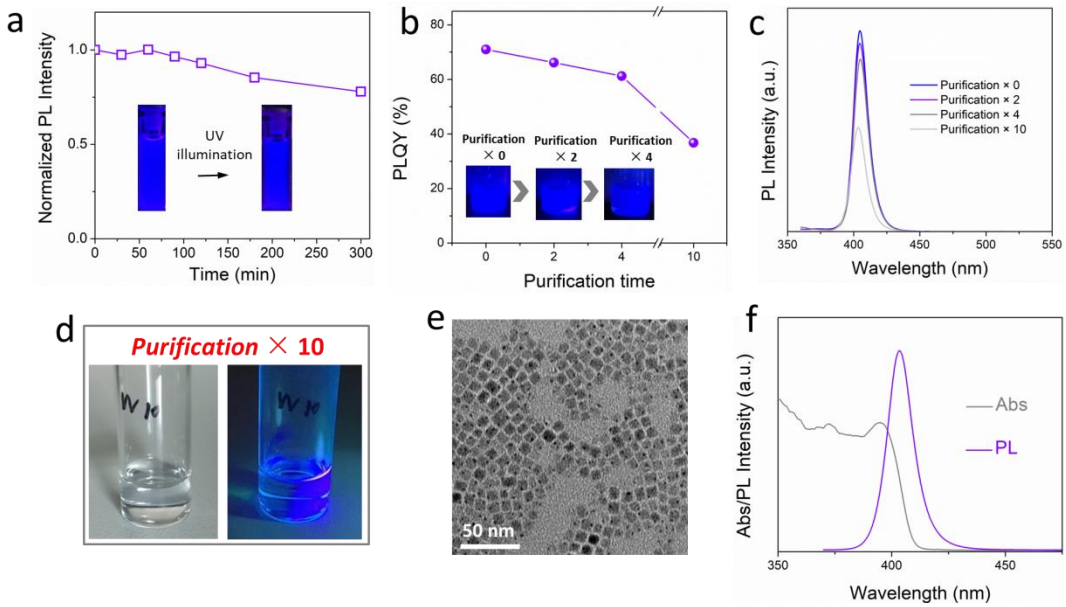

Figure 2. (a) Normalized PL intensity of the $PhPOCl_2$ based $CsPbCl_3$ NCs under continuous high-power UV light illumination (inset: corresponding photograph under UV light before and after UV light illumination). (b) PLQY (inset: corresponding photograph under UV light before and after purification cycles) and (c) PL spectra of the $PhPOCl_2$ based $CsPbCl_3$ NCs before and after different cycles of purifications with anti-solvent. (d) The photographs under daylight and UV light, (e) TEM image, and (f) optical absorption and PL spectra (excitation wavelength 350 nm) of the $PhPOCl_2$ based $CsPbCl_3$ NCs after 10 cycles of purifications.

Furthermore, our $PhPOCl_2$ based $CsPbCl_3$ NCs show robust stability against light irradiation and repeated purification. **Figure 2a** shows the measured photo-stability results of $PhPOCl_2$ based $CsPbCl_3$ NCs (purified sample) under continuous illumination with a high power UV light (365 nm, 8 W/cm^2). Its PL intensity remained almost 80% of the iniatate value after 5 h, which was significantly better than the $CsPbCl_3$ NCs synthesized from other reported Cl precursors (**Figure S5**). For optoelectronic device applications, the appropriate purification steps are necessary to remove the excess insulating organic ligands of NCs with the assistance of anti-solvents, which yet often deteriorates the optical property and device performance of

semiconductor NCs (especially the vulnerable $CsPbCl_3$ NCs).[47] With this in mind, we purify $PhPOCl_2$ based $CsPbCl_3$ NCs repeatedly with acetonitrile, a relatively high polar solvent, as the anti-solvent. As shown in **Figure 2b**, the $PhPOCl_2$ based $CsPbCl_3$ NCs were still highly luminescent after four cycles of purification. In comparison, the absolute PLQY value decreased to 66.2%, which was 86% of the value before purification (71%). No PL spectra shift and shape change were observed (**Figure 2c**). Additionally, the XRD pattern and TEM image of $CsPbCl_3$ NCs after purification were obtained (**Figure S6**). After 4 cycles of purifications, the $PhPOCl_2$ based $CsPbCl_3$ NCs maintained the original crystal structure and NC morphology. The above results clearly reveal that our $PhPOCl_2$ based $CsPbCl_3$ NCs exhibite an excellent stability against repeated purification process. The distinctive superiority of the $PhPOCl_2$ based $CsPbCl_3$ NCs is further demonstrated through the direct compasion with the $CsPbCl_3$ NCs synthesized from other reported Cl precursors (see detail in **Figure S7)**. In addition, the Fourier-transform infrared (FTIR) spectra of our $PhPOCl_2$ based $CsPbCl_3$ NCs before and after purification (**Figure S8**) clearly show that the absorption intensity of organic ligands gradually reduced after purification cycles, thus suggesting the successful and effective purification process.

Considering the excellent stability of our $PhPOCl_2$ based $CsPbCl_3$ NCs, we further purified them for 10 cycles using the same procedure. Remarkably the NCs sample still showed bright luminescence with good colloidal stability (**Figure 2d**). The TEM and XRD results also confirmed that the NC size, shape, and crystal structure were almost unchanged, and no other impurity phases were observed (**Figure 2e and Figure S9**). As shown in **Figure 2f**, the $CsPbCl_3$ NCs with 10 cycles of purification still exhibit distinct exciton absorption and bright PL peak (403 nm), even though the absolute PLQY value decreased to 36.8% (**Figure 2b and Figure**

S10). These results further highlight the potential of our $PhPOCl_2$ synthesis route toward clean $CsPbCl_3$ NCs with high quality optoelectronic properties.

We performed further investigations to gain more insights into the mechanisms responsible for the observed excellent optical properties and unprecedented stability of $PhPOCl_2$ based $CsPbCl_3$ NCs. As we know, despite the acknowledged defect tolerance merit of lead halide perovskite materials, the surface capping ligands of perovskite NCs play a crucial role in optoelectronic properties and stability.[48-49] Considering the uniform NC size, morphology, and crystal structure of the $PhPOCl_2$ based $CsPbCl_3$ NCs compared to the reported samples, we hypothesize that the high-quality $PhPOCl_2$ based $CsPbCl_3$ NCs could be attributed to their distinct surface chemistry because of the P=O containing Cl precursor that was used. According to many previous reports, P=O can regulate the perovskite NC surface through either (1) direct passivation with lead (P=O:Pb), or (2) alter the binding motif of original ligands (OA and/or OLA) on the NC surface.[46, 50-51] To clarify whether P=O binds directly on the NC surface, we employed the FTIR and nuclear magnetic resonance (NMR) spectroscopic techniques for characterization. The FTIR spectra of $PhPOCl_2$ and the as-synthesized $CsPbCl_3$ NCs are shown in **Figure S11**. For $PhPOCl_2$, the strong absorption band at 1439 and 1270 cm^{-1} can be assigned to the P-Ph and P=O stretching vibration modes, respectively. The peaks at 680-750 cm^{-1} are the characteristic signal of the benzene ring.[52] But we did not observe any of these typical peaks of $PhPOCl_2$ on the $CsPbCl_3$ NC sample. These results suggest that the $PhPOCl_2$ precursor was absent on the NC and thus exclude the possible passivation effect of P=O on the $CsPbCl_3$ NC surface. Furthermore, the ^{31}P NMR spectrum of $CsPbCl_3$ NC sample was shown in **Figure S12**, which also confirms the absence of any P signal on the $CsPbCl_3$ NCs. Therefore, in our reaction

system, instead of acting as a passivating ligand, $PhPOCl_2$ (featuring P=O) is a surface regulator for the $CsPbCl_3$ NCs.

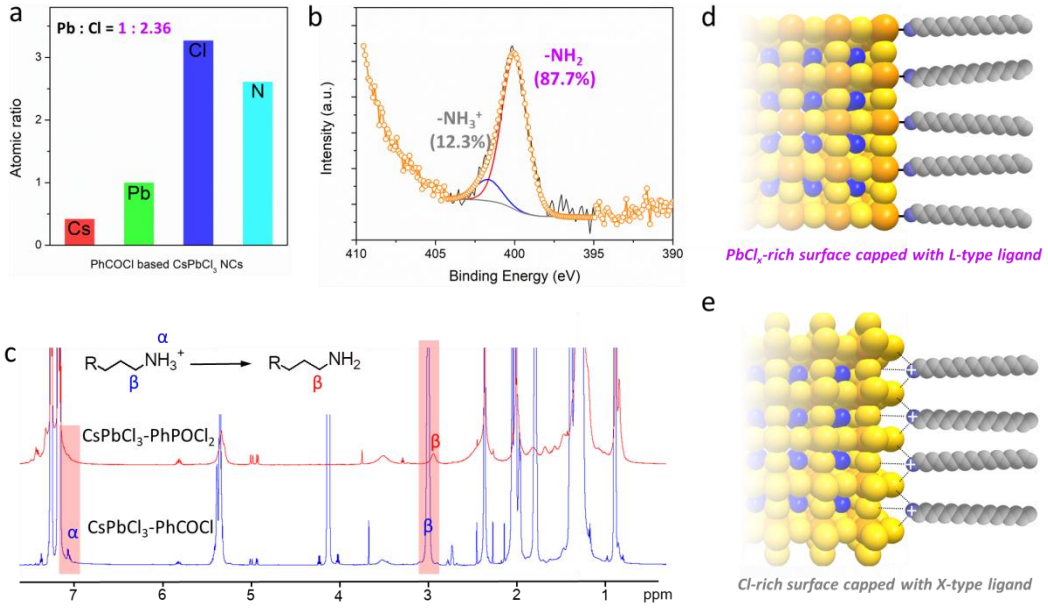

Figure 3. (a) Calculated atomic ratio and (b) high-resolution XPS spectra of N 1s of the $PhPOCl_2$ based $CsPbCl_3$ NCs. (c) ^1H NMR spectra of the PhCOCl and $PhPOCl_2$ based $CsPbCl_3$ NCs. Schematic of $CsPbCl_3$ NC with (d) $PbCl_x$-rich surface capped with L-type OLA ligand and (e) Cl-rich surface capped with X-type $OLAH^+$ ligand.

In general, using common synthesis approaches with the assistance of OA and OLA ligands, it is well accepted that the formed perovskite NCs are terminated with a halide-rich surface and an X-type binding motif in which the protonated OLA cations ($OLAH^+$) bind with the surface halide anions.[53-54] According to the mutual equilibrium (OA^- (Cl^-) + $OLAH^+$ ⇋ OLA + OA (HCl)), these ionic ligands are prone to rapid desorption from the NC surface, giving rise to the generation of trap states (e.g., Cl-vacancy defects) or even phase change.[55] To investigate the NC surface chemistry and ligand binding, we performed X-ray photoelectron spectroscopy (XPS), NMR and FTIR measurements. As shown in **Figure S13**, the core-level signal of Cs 3d, Pb 4f,

and Cl 2p can be observed in the full XPS spectra of the $PhPOCl_2$ based $CsPbCl_3$ NC sample. The atomic ratio of Cs:Pb:Cl was calculated to be 0.5:1:2.36 (**Figure 3a**), of which the Cl/Pb molar ratio is much lower than stoichiometry (3:1) and the reported PhCOCl based $CsPbCl_3$ NC sample (3.27:1) (**Figure S14**). This result revealed that $PhPOCl_2$ based $CsPbCl_3$ NCs have a $PbCl_x$-rich surface, instead of the prevalent halide-rich surface of the perovskite NCs obtained from the halide-rich synthesis approaches. **Figure 3b** shows the high-resolution XPS spectra of the N 1s core level of $PhPOCl_2$ based $CsPbCl_3$ NC sample, which can be divided into two components at 400 and 402 eV, corresponding to the terminal amine groups ($-NH_2$) and protonated amine groups ($-NH_3^+$), respectively.[56] Importantly, the non-protonated $-NH_2$ accounts for 87.7% of the surface amine ligands on $PhPOCl_2$ based $CsPbCl_3$ NCs. In contrast, the ratio of $-NH_2$ in the PhCOCl based $CsPbCl_3$ NC sample is only 31.2% (**Figure S15**). Based on the observed $PbCl_x$-rich and the predominant $-NH_2$ terminal groups on the NC surface, we can conclude that in our case, the $CsPbCl_3$ NCs are mainly capped with the L-type OLA ligand, rather than the protonated $OLAH^+$ ionic ligands.[57] This point can be further identified by the NMR characterization result. As shown in **Figure 3c**, the peaks α at 7.1 ppm of the PhCOCl based $CsPbCl_3$ NC sample can be explicitly ascribed to the bound $OLAH^+$ on NC surface, in which the feature of multiple peaks with sharp splitting could be explained by the restricted mutual proton exchanges of ammonium protons.[58] Contrastingly, no signal of this kind of ammonium protons was found for our $PhPOCl_2$ based $CsPbCl_3$ NC sample. In addition, the ^1H resonances β of the PhCOCl based $CsPbCl_3$ NC sample located at 3.0 ppm is the typical signal of α-CH_2 of oleylammonium,[55, 57] which was clearly observed to upshift to 2.94 ppm for the $PhPOCl_2$ based $CsPbCl_3$ NC sample. These results which match well with previous report

demonstrated the change of binding ligand from protonated $OLAH^+$ to non-protonated OLA when the $PhPOCl_2$ was used as Cl precursor, schematically illustrated in **Figure 3d-e.**

As we mentioned above, the $PhPOCl_2$ precursor we used in the synthesis process of $CsPbCl_3$ NCs is an surface regulator agent for the $CsPbCl_3$ NCs. But how does the $PhPOCl_2$ precursor link the distinct NC surface and ligand passivation motif? Recently, Almeida *et al.* [50] and Ashton *et al.* [51] demonstrated a phosphine oxide route for the synthesis of $CsPbBr_3$ and $FAPbBr_3$ NCs, respectively, by utilization of trioctylphosphine oxide (TOPO) that featuring P=O as well. In these works, the significant role of TOPO in the perovskite NC synthesis process was based on the acid-base interaction of OA and TOPO, namely the proton affinity of P=O in TOPO. With this in mind, we hypothesize that the $PhPOCl_2$ precursor featuring P=O in our reaction is able to interact with the acidic protons as well that greatly suppress the protonation of OLA, thus promoting the L-type OLA ligand capped on the $CsPbCl_3$ NCs. To verify this point, the interaction between $PhPOCl_2$ derived P=O in our reaction system and OA was investigated through the ^{31}P NMR spectra. We should note that the diphenylphosphine oxide (DPPO) was employed here to replace the $PhPOCl_2$ and avoid the interference of the highly reactive P-Cl. As shown in **Figure S16**, compared to the pure DPPO, the presence of OA promoted the ^{31}P signal shift downfield, suggesting the deshielding effect of the probe nuclei that could be attributed to the protonation of P=O with acid protons. To gain more insights, we tracked the temperature-dependent ^{31}P NMR spectra based on the pure DPPO and DPPO/OA (1:1 molar ratio) samples. When the temperature increased from 15 ℃ to 75 ℃, the ^{31}P signal of DPPO shift upfield gradually. In DPPO/OA mixture sample, it shifted upfield as well and but to a greater extend. These results are in line with the previous observation in the TOPO/OA system,[50-51] which clearly demonstrates the exothermic feature of acid-base interaction between DPPO and OA,

thus further confirm the protonation of P=O in our $CsPbCl_3$ NCs synthesis reaction and rationalize the derived distinct NC surface termination and L-type ligand binding feature. Accordingly, compared with the weak binding of X-type ligands $OLAH^+$ with Cl anions on $CsPbCl_3$ NC surface (hydrogen bonding), the non-protonated L-type ligands OLA in our case are able to strongly bind with lead atoms of NC surface via covalent bond, also should provide fully delocalized valence band maximum (VBM) and conduction band minimum (CBM) states.[57] Therefore, we can conclude here that in our $PhPOCl_2$ based synthesis approach, as depicted in **Figure S17**, except as the Cl precursor for $CsPbCl_3$ NC nucleation and growth, the excess of P=O of $PhPOCl_2$ in our reaction can suppress the protonation of OLA, promoting the non-protonated L-type OLA strongly bind on the NC surface through covalent bond, thus leading to the significantly improved optical quality and unprecedented stability.

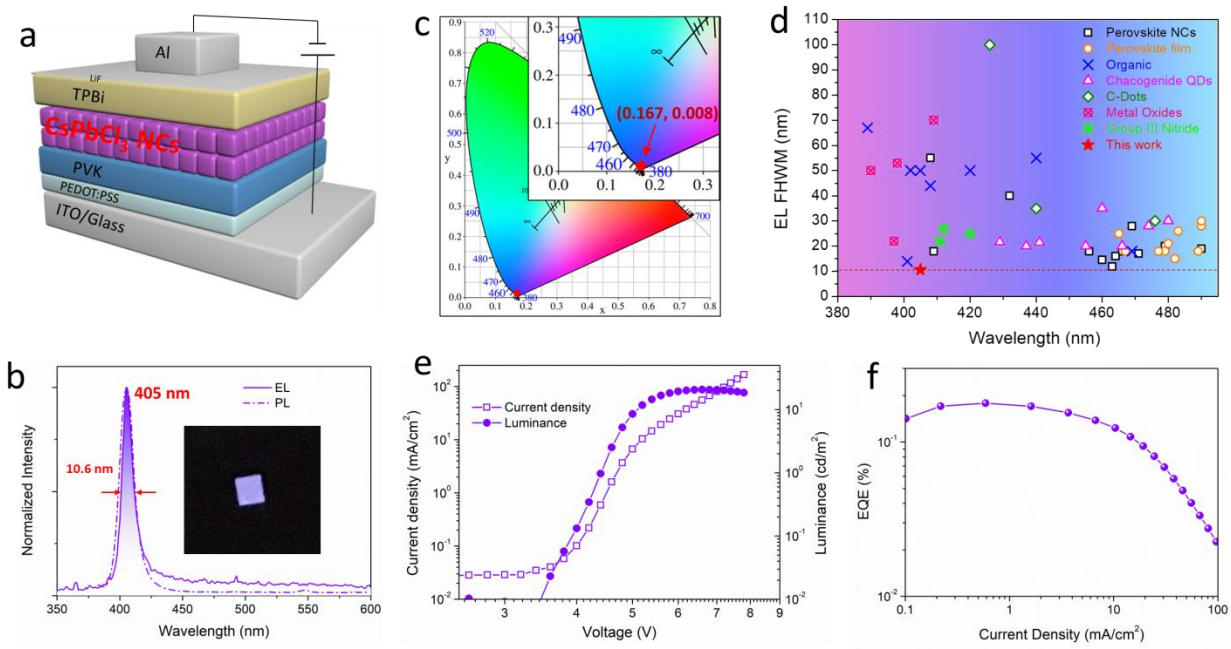

Figure 4. (a) Schematic drawing showing the device structure, (b) normalized PL and EL spectra (Insert shows a photograph of a working device), and (c) corresponding CIE coordinates of the $PhPOCl_2$ based $CsPbCl_3$ NCs LED. (d) Summary of the EL peak wavelength and FWHM of

visible LEDs spanning from ultraviolet to blue range, based on emitting materials of perovskite NCs,[18-19, 21-22, 34, 49, 59-63] perovskite film,[17, 20, 46, 64-69] organic solids,[2, 9, 12-13, 70-73] chalcogenide QDs,[10, 14, 74-79] carbon-dots,[15, 80-81] metal oxides,[7-8, 82] group III nitrides.[11, 83] (e) Current density and luminance versus driving voltage curves. (f) EQE versus current density curve of the as-fabricated LED.

Finally, as a demonstration of our high quality $CsPbCl_3$ NCs as active materials for violet LEDs, we fabricated the planar device with the architecture depicted in **Figure 4a**. More specifically, $PhPOCl_2$ based $CsPbCl_3$ NCs after 10 cycles of purification were employed as the emitting materials. The corresponding flat-band energy diagram was shown in **Figure S18**, in which the VBM and CBM of $CsPbCl_3$ NCs emitting layer were estimated from the ultraviolet photoemission spectroscopy (UPS) (**Figure S19**). The poly(3,4-ethylenedioxythiophene) polystyrene sulfonate (PEDOT:PSS), polyvinylcarbazole (PVK) and (1-phenyl-1 H-benzimidazol-2-yl)benzene (TPBi) was used as the hole injection layer, hole transport layer and electron transport layer respectively. Initially, the morphology of the fabricated PVK and $CsPbCl_3$ NC films were checked through atomic force microscopy (AFM) technique. As shown in **Figure S20**, both of them show the uniform and flat film morphology with a much low root mean square roughness of 0.54 nm and 1.82 nm, respectively. **Figure 4b** shows the EL spectra of $CsPbCl_3$ NC based LED, featuring an extremely sharp peak at 405 nm with FWHM of 10.6 nm. For comoparsion, the PL spectra of the $CsPbCl_3$ NC film are also presented, which confirm that the emission of LED was originated from the $CsPbCl_3$ NCs, rather than other species. As shown in **Figure S21**, the EL spectra under different voltages exhibited unchanged shape and peak position, which clearly confirmed that the EL was originated from the $CsPbCl_3$ NCs layer. The corresponding Commission Internationale de l'Eclairage (CIE) coordinates were calculated to be

(0.167, 0.008) (**Figure 4c**). We should note that the y-color coordinate that below 0.01 is the smallest value of almost all reported visible LEDs. To give a straightforward view, we directly compared the EL emission wavelength and FWHM of the state-of-the-art reported LEDs spanning from ultraviolet to blue range. It is obvious that our $CsPbCl_3$ NCs based LED exhibits the smallest EL FWHM among them, which greatly highlights their ultrapure EL emission (**Figure 4d**). The luminance and current density curves as a function of applied voltage were presented in **Figure 4e,** which shows a turn-on voltage of ~3.6 V of $CsPbCl_3$ NCs based LED. The maximum luminance reached 21 cd/m^2. The maximum EQE was calculated to be 0.18% at the current density of ~0.6 mA/cm^2 (**Figure 4f**), which is comparable with the best-performing violet LEDs based on metal halide perovskites, but with the shortest EL emission wavelength and smallest EL FWHM.[19-20, 22] The great difficulties to the access of high PLQY (up to near-unity) of $CsPbCl_3$ stem from the defect states originated from both the Cl vacancies and the undesired tilting of the octahedral units.[38, 41] From this point, we envisage that except for the surface engineering, the optical quality, stability, and device performance of $CsPbCl_3$ NCs can be further improved through composition engineering such as B-site doping. On the other hand, considering the relatively large bandgap of $CsPbCl_3$ NCs, the mismatched energy alignment causing insufficient charge carrier injection is likely another obstacle toward the high device performance. Therefore, in future works, it is desirable to optimize the device structure with more efficient charge injection.

In summary, we have developed an efficient approach to synthesize high quality violet emitting $CsPbCl_3$ NCs with unprecedented stability by using $PhPOCl_2$ as a novel Cl precursor. The detailed surface chemistry investigations reveal that the benefit of the new synthesis approach lies in the promoted generation of the non-protonated L-type capping ligand (OLA)

with strong covalent binding. Using the highly stable $CsPbCl_3$ NCs as emitting material, we realized the efficient violet LED with extremely narrow EL spectrum of which the FWHM is smaller than all the previously reported visible and even ultraviolet LEDs. Our synthesis approach opens a new avenue for producing full-Cl based perovskite nanomaterials and holds great promise for the realization of ultrapure LEDs via solution processing.

ASSOCIATED CONTENT

Supporting Information. Additional TEM images, UV-vis absorption spectra, PL spectra, XPS spectra, XRD patterns, FTIR spectra, NMR spectra, and UPS spectra of the $CsPbCl_3$ NCs; AFM images of PVK and $CsPbCl_3$ NC film; EL spectra of the $CsPbCl_3$ NC-LED.

AUTHOR INFORMATION

Corresponding Authors

*Yabing.Qi@OIST.jp

*liangli117@sjtu.edu.cn

Notes

The authors declare no competing financial interest.

ACKNOWLEDGMENT

This work was supported by the Guangdong Province's 2018-2019 Key R&D Program (2019B010924001), the National Key Research and Development Program (No. 2017YFE0127100), National Natural Science Foundation of China (NSFC21773155), Shanghai Sailing Program (19YF1422200). This work was also supported by the funding from the Energy

Materials and Surface Sciences Unit of the Okinawa Institute of Science and Technology Graduate University, the OIST R&D Cluster Research Program, the OIST Proof of Concept (POC) Program, and JST A-STEP Grant Number JPMJTM20HS, Japan.

REFERENCES

(1) Khan, A.; Balakrishnan, K.; Katona, T., Ultraviolet light-emitting diodes based on group three nitrides. *Nat. Photonics* **2008,** *2* (2), 77-84.

(2) Chao, T. C.; Lin, Y. T.; Yang, C. Y.; Hung, T. S.; Chou, H. C.; Wu, C. C.; Wong, K. T., Highly efficient UV organic light-emitting devices based on Bi(9, 9-diarylfluorene)s. *Adv. Mater.* **2005,** *17* (8), 992-996.

(3) Lembo, A. J.; Ganz, R. A.; Sheth, S.; Cave, D.; Kelly, C.; Levin, P.; Kazlas, P. T.; Baldwin III, P. C.; Lindmark, W. R.; McGrath, J. R.; et al., Treatment of Helicobacter pylori infection with intra-gastric violet light phototherapy: A pilot clinical trial. *Lasers Surg. Med.* **2009,** *41* (5), 337-344.

(4) Nakamura, S., InGaN-based violet laser diodes. *Semicond. Sci. Technol.* **1999,** *14* (6), R27-R40.

(5) Du, X.; Mei, Z.; Liu, Z.; Guo, Y.; Zhang, T.; Hou, Y.; Zhang, Z.; Xue, Q.; Kuznetsov, A. Y., Controlled growth of high-quality ZnO-based films and fabrication of visible-blind and solar-blind ultra-violet detectors. *Adv. Mater.* **2009,** *21* (45), 4625-4630.

(6) Hwang, D.-K.; Kang, S.-H.; Lim, J.-H.; Yang, E.-J.; Oh, J.-Y.; Yang, J.-H.; Park, S.-J., p-ZnO/n-GaN heterostructure ZnO light-emitting diodes. *Appl. Phys. Lett.* **2005,** *86* (22), 222101.

(7) Lupan, O.; Pauporté, T.; Viana, B., Low-voltage UV-electroluminescence from ZnO-Nanowire array/p-GaN light-emitting diodes. *Adv. Mater.* **2010,** *22* (30), 3298-3302.

(8) Brovelli, S.; Chiodini, N.; Lorenzi, R.; Lauria, A.; Romagnoli, M.; Paleari, A., Fully inorganic oxide-in-oxide ultraviolet nanocrystal light emitting devices. *Nat. Commun.* **2012,** *3* (1), 1-9.

(9) Chen, W.-C.; Yuan, Y.; Ni, S.-F.; Tong, Q.-X.; Wong, F.-L.; Lee, C.-S., Achieving efficient violet-blue electroluminescence with CIEy < 0.06 and EQE > 6% from naphthyl-linked phenanthroimidazole-carbazole hybrid fluorophores. *Chem. Sci.* **2017,** *8* (5), 3599-3608.

(10) Kwak, J.; Lim, J.; Park, M.; Lee, S.; Char, K.; Lee, C., High-power genuine ultraviolet light-emitting diodes based on colloidal nanocrystal quantum dots. *Nano Lett.* **2015,** *15* (6), 3793-3799.

(11) Nakamura, S.; Senoh, M.; Mukai, T., High-power InGaN/GaN double-heterostructure violet light emitting diodes. *Appl. Phys. Lett.* **1993,** *62* (19), 2390-2392.

(12) Zhang, Q.; Li, J.; Shizu, K.; Huang, S.; Hirata, S.; Miyazaki, H.; Adachi, C., Design of efficient thermally activated delayed fluorescence materials for pure blue organic light emitting diodes. *J. Am. Chem. Soc.* **2012,** *134* (36), 14706-14709.

(13) Luo, Y.; Li, S.; Zhao, Y.; Li, C.; Pang, Z.; Huang, Y.; Yang, M.; Zhou, L.; Zheng, X.; Pu, X.; et al., An Ultraviolet Thermally Activated Delayed Fluorescence OLED with Total External Quantum Efficiency over 9%. *Adv. Mater.* **2020,** *32* (32), 2001248.

(14) Shen, H.; Cao, W.; Shewmon, N. T.; Yang, C.; Li, L. S.; Xue, J., High-efficiency, low turn-on voltage blue-violet quantum-dot-based light-emitting diodes. *Nano Lett.* **2015,** *15* (2), 1211-1216.

(15) Yuan, F.; Wang, Y.-K.; Sharma, G.; Dong, Y.; Zheng, X.; Li, P.; Johnston, A.; Bappi, G.; Fan, J. Z.; Kung, H.; et al., Bright high-colour-purity deep-blue carbon dot light-emitting diodes via efficient edge amination. *Nat. Photonics* **2020,** *14* (3), 171-176.

(16) Sadhanala, A.; Ahmad, S.; Zhao, B.; Giesbrecht, N.; Pearce, P. M.; Deschler, F.; Hoye, R. L.; Gödel, K. C.; Bein, T.; Docampo, P.; et al., Blue-green color tunable solution processable organolead chloride-bromide mixed halide perovskites for optoelectronic applications. *Nano Lett.* **2015,** *15* (9), 6095-6101.

(17) Li, Z. C.; Chen, Z. M.; Yang, Y. C.; Xue, Q. F.; Yip, H. L.; Cao, Y., Modulation of recombination zone position for quasi-two-dimensional blue perovskite light-emitting diodes with efficiency exceeding 5%. *Nat. Commun.* **2019,** *10*, 1027.

(18) Hou, S. C.; Gangishetty, M. K.; Quan, Q. M.; Congreve, D. N., Efficient Blue and White Perovskite Light-Emitting Diodes via Manganese Doping. *Joule* **2018,** *2* (11), 2421-2433.

(19) Ma, Z.; Shi, Z.; Yang, D.; Zhang, F.; Li, S.; Wang, L.; Wu, D.; Zhang, Y.; Na, G.; Zhang, L.; et al., Electrically-driven violet light-emitting devices based on highly stable lead-free perovskite $Cs_3Sb_2Br_9$ quantum dots. *ACS Energy Lett.* **2019,** *5* (2), 385-394.

(20) Liang, D.; Peng, Y.; Fu, Y.; Shearer, M. J.; Zhang, J.; Zhai, J.; Zhang, Y.; Hamers, R. J.; Andrew, T. L.; Jin, S., Color-pure violet-light-emitting diodes based on layered lead halide perovskite nanoplates. *ACS Nano* **2016,** *10* (7), 6897-6904.

(21) Zhang, C. Y.; Wan, Q.; Wang, B.; Zheng, W. L.; Liu, M. M.; Zhang, Q. G.; Kong, L.; Li, L., Surface Ligand Engineering toward Brightly Luminescent and Stable Cesium Lead Halide Perovskite Nanoplatelets for Efficient Blue-Light-Emitting Diodes. *J. Phys. Chem. C* **2019,** *123* (43), 26161-26169.

(22) Deng, W.; Jin, X.; Lv, Y.; Zhang, X.; Zhang, X.; Jie, J., 2D Ruddlesden-Popper Perovskite Nanoplate Based Deep-Blue Light-Emitting Diodes for Light Communication. *Adv. Funct. Mater.* **2019,** *29* (40), 1903861.

(23) Tan, Z.-K.; Moghaddam, R. S.; Lai, M. L.; Docampo, P.; Higler, R.; Deschler, F.; Price, M.; Sadhanala, A.; Pazos, L. M.; Credgington, D.; et al., Bright light-emitting diodes based on organometal halide perovskite. *Nat. Nanotechnol.* **2014,** *9* (9), 687-692.

(24) Akkerman, Q. A.; D'Innocenzo, V.; Accornero, S.; Scarpellini, A.; Petrozza, A.; Prato, M.; Manna, L., Tuning the optical properties of cesium lead halide perovskite nanocrystals by anion exchange reactions. *J. Am. Chem. Soc.* **2015,** *137* (32), 10276-10281.

(25) Wang, N.; Cheng, L.; Ge, R.; Zhang, S.; Miao, Y.; Zou, W.; Yi, C.; Sun, Y.; Cao, Y.; Yang, R.; et al., Perovskite light-emitting diodes based on solution-processed self-organized multiple quantum wells. *Nat. Photonics* **2016,** *10* (11), 699.

(26) Shang, Y.; Liao, Y.; Wei, Q.; Wang, Z.; Xiang, B.; Ke, Y.; Liu, W.; Ning, Z., Highly stable hybrid perovskite light-emitting diodes based on Dion-Jacobson structure. *Science Advances* **2019,** *5* (8), eaaw8072.

(27) Cao, Y.; Wang, N.; Tian, H.; Guo, J.; Wei, Y.; Chen, H.; Miao, Y.; Zou, W.; Pan, K.; He, Y.; et al., Perovskite light-emitting diodes based on spontaneously formed submicrometre-scale structures. *Nature* **2018,** *562* (7726), 249.

(28) Shen, Y.; Li, M.-N.; Li, Y.; Xie, F.-M.; Wu, H.-Y.; Zhang, G.-H.; Chen, L.; Lee, S.-T.; Tang, J.-X., Rational interface engineering for efficient flexible perovskite light-emitting diodes. *ACS Nano* **2020,** *14* (5), 6107-6116.

(29) Xu, W. D.; Hu, Q.; Bai, S.; Bao, C. X.; Miao, Y. F.; Yuan, Z. C.; Borzda, T.; Barker, A. J.; Tyukalova, E.; Hu, Z. J.; et al., Rational molecular passivation for high-performance perovskite light-emitting diodes. *Nat. Photonics* **2019,** *13* (6), 418-424.

(30) Xiao, Z.; Kerner, R.; Zhao, L.; Tran, N.; Lee, K., Efficient perovskite light-emitting diodes featuring nanometre-sized crystallites. *Nat. Photonics* **2017,** *11* (2), 108-115.

(31) Cho, H.; Jeong, S.-H.; Park, M.-H.; Kim, Y.-H.; Wolf, C.; Lee, C.-L.; Heo, J. H.; Sadhanala, A.; Myoung, N.; Yoo, S.; et al., Overcoming the electroluminescence efficiency limitations of perovskite light-emitting diodes. *Science* **2015,** *350* (6265), 1222-1225.

(32) Chih, Y. K.; Wang, J. C.; Yang, R. T.; Liu, C. C.; Chang, Y. C.; Fu, Y. S.; Lai, W. C.; Chen, P.; Wen, T. C.; Huang, Y. C.; et al., NiO_x electrode interlayer and $CH_3NH_2/CH_3NH_3PbBr_3$ Interface treatment to markedly advance hybrid perovskite-based light-emitting diodes. *Adv. Mater.* **2016,** *28* (39), 8687-8694.

(33) Qin, C.; Matsushima, T.; Potscavage, W. J.; Sandanayaka, A. S.; Leyden, M. R.; Bencheikh, F.; Goushi, K.; Mathevet, F.; Heinrich, B.; Yumoto, G.; et al., Triplet management for efficient perovskite light-emitting diodes. *Nat. Photonics* **2020,** *14* (2), 70-75.

(34) Dong, Y.; Wang, Y.-K.; Yuan, F.; Johnston, A.; Liu, Y.; Ma, D.; Choi, M.-J.; Chen, B.; Chekini, M.; Baek, S.-W.; et al., Bipolar-shell resurfacing for blue LEDs based on strongly confined perovskite quantum dots. *Nat. Nanotechnol.* **2020,** *15* (8), 668-674.

(35) Pina, J. M.; Parmar, D. H.; Bappi, G.; Zhou, C.; Choubisa, H.; Vafaie, M.; Najarian, A. M.; Bertens, K.; Sagar, L. K.; Dong, Y.; et al., Deep-Blue Perovskite Single-Mode Lasing through Efficient Vapor-Assisted Chlorination. *Adv. Mater.* **2020,** *33*, 2006697.

(36) Dutta, A.; Behera, R. K.; Pal, P.; Baitalik, S.; Pradhan, N., Near-Unity Photoluminescence Quantum Efficiency for All $CsPbX_3$ (X = Cl, Br, and I) Perovskite Nanocrystals: A Generic Synthesis Approach. *Angew. Chem. Int. Ed.* **2019,** *58* (17), 5552-5556.

(37) Protesescu, L.; Yakunin, S.; Bodnarchuk, M. I.; Krieg, F.; Caputo, R.; Hendon, C. H.; Yang, R. X.; Walsh, A.; Kovalenko, M. V., Nanocrystals of cesium lead halide perovskites ($CsPbX_3$, X= Cl, Br, and I): novel optoelectronic materials showing bright emission with wide color gamut. *Nano Lett.* **2015,** *15* (6), 3692-3696.

(38) Yong, Z.-J.; Guo, S.-Q.; Ma, J.-P.; Zhang, J.-Y.; Li, Z.-Y.; Chen, Y.-M.; Zhang, B.-B.; Zhou, Y.; Shu, J.; Gu, J.-L.; et al., Doping-enhanced short-range order of perovskite nanocrystals for near-unity violet luminescence quantum yield. *J. Am. Chem. Soc.* **2018,** *140* (31), 9942-9951.

(39) Ahmed, G. H.; El-Demellawi, J. K.; Yin, J.; Pan, J.; Velusamy, D. B.; Hedhili, M. N.; Alarousu, E.; Bakr, O. M.; Alshareef, H. N.; Mohammed, O. F., Giant photoluminescence

enhancement in $CsPbCl_3$ perovskite nanocrystals by simultaneous dual-surface passivation. *ACS Energy Lett.* **2018,** *3* (10), 2301-2307.

(40) Imran, M.; Caligiuri, V.; Wang, M. J.; Goldoni, L.; Prato, M.; Krahne, R.; De Trizio, L.; Manna, L., Benzoyl Halides as Alternative Precursors for the Colloidal Synthesis of Lead-Based Halide Perovskite Nanocrystals. *J. Am. Chem. Soc.* **2018,** *140* (7), 2656-2664.

(41) Mondal, N.; De, A.; Samanta, A., Achieving Near-Unity Photoluminescence Efficiency for Blue-Violet-Emitting Perovskite Nanocrystals. *ACS Energy Lett.* **2019,** *4* (1), 32-39.

(42) De, A.; Das, S.; Mondal, N.; Samanta, A., Highly luminescent violet-and blue-emitting stable perovskite nanocrystals. *ACS Mater. Lett.* **2019,** *1* (1), 116-122.

(43) Behera, R. K.; Das Adhikari, S.; Dutta, S. K.; Dutta, A.; Pradhan, N., Blue-emitting $CsPbCl_3$ nanocrystals: impact of surface passivation for unprecedented enhancement and loss of optical emission. *J. Phys. Chem. Lett.* **2018,** *9* (23), 6884-6891.

(44) Imai, Y.; Kamata, H.; Kakimoto, M. A., Preparation and properties of high transition temperature aromatic polyphosphonates by phase-transfer-catalyzed polycondensation of phenylphosphonic dichloride with bisphenols. *J. Polym. Sci., Part A: Polym. Chem.* **1984,** *22* (6), 1259-1265.

(45) Busch, H.; Majumder, S.; Reiter, G. n.; Mecking, S., Semicrystalline Long-Chain Polyphosphoesters from Polyesterification. *Macromolecules* **2017,** *50* (7), 2706-2713.

(46) Ma, D.; Todorovic, P.; Meshkat, S.; Saidaminov, M.; Wang, Y.-K.; Chen, B.; Li, P.; Scheffel, B.; Quintero-Bermudez, R.; Fan, J. Z.; et al., Chloride Insertion-Immobilization Enables Bright, Narrowband, and Stable Blue-Emitting Perovskite Diodes. *J. Am. Chem. Soc.* **2020,** *142* (11), 5126-5134.

(47) Nenon, D. P.; Pressler, K.; Kang, J.; Koscher, B. A.; Olshansky, J. H.; Osowiecki, W. T.; Koc, M. A.; Wang, L.-W.; Alivisatos, A. P., Design Principles for Trap-Free CsPbX3 Nanocrystals: Enumerating and Eliminating Surface Halide Vacancies with Softer Lewis Bases. *J. Am. Chem. Soc.* **2018,** *140* (50), 17760-17772.

(48) Park, J.; Jang, H. M.; Kim, S.; Jo, S. H.; Lee, T.-W., Electroluminescence of Perovskite Nanocrystals with Ligand Engineering. *Trends Chem.* **2020,** *2* (9), 837-849.

(49) Pan, J.; Quan, L. N.; Zhao, Y.; Peng, W.; Murali, B.; Sarmah, S. P.; Yuan, M.; Sinatra, L.; Alyami, N. M.; Liu, J.; et al., Highly Efficient Perovskite-Quantum-Dot Light-Emitting Diodes by Surface Engineering. *Adv. Mater.* **2016,** *28* (39), 8718-8725.

(50) Almeida, G.; Ashton, O. J.; Goldoni, L.; Maggioni, D.; Petralanda, U.; Mishra, N.; Akkerman, Q. A.; Infante, I.; Snaith, H. J.; Manna, L., The Phosphine Oxide Route toward Lead Halide Perovskite Nanocrystals. *J. Am. Chem. Soc.* **2018,** *140* (44), 14878-14886.

(51) Ashton, O. J.; Marshall, A. R.; Warby, J. H.; Wenger, B.; Snaith, H. J., A phosphine oxide route to formamidinium lead tribromide nanoparticles. *Chem. Mater.* **2020,** *32* (17), 7172-7180.

(52) Zhu, C.; He, M.; Cui, J.; Tai, Q.; Song, L.; Hu, Y., Synthesis of a novel hyperbranched and phosphorus-containing charring-foaming agent and its application in polypropylene. *Polym. Adv. Technol.* **2018,** *29* (9), 2449-2456.

(53) De Roo, J.; Ibáñez, M.; Geiregat, P.; Nedelcu, G.; Walravens, W.; Maes, J.; Martins, J. C.; Van Driessche, I.; Kovalenko, M. V.; Hens, Z., Highly dynamic ligand binding and light absorption coefficient of cesium lead bromide perovskite nanocrystals. *ACS Nano* **2016,** *10* (2), 2071-2081.

(54) Ravi, V. K.; Santra, P. K.; Joshi, N.; Chugh, J.; Singh, S. K.; Rensmo, H.; Ghosh, P.; Nag, A., Origin of the substitution mechanism for the binding of organic ligands on the surface of $CsPbBr_3$ perovskite nanocubes. *J. Phys. Chem. Lett.* **2017,** *8* (20), 4988-4994.

(55) Almeida, G.; Goldoni, L.; Akkerman, Q.; Dang, Z.; Khan, A. H.; Marras, S.; Moreels, I.; Manna, L., Role of acid-base equilibria in the size, shape, and phase control of cesium lead bromide nanocrystals. *ACS Nano* **2018,** *12* (2), 1704-1711.

(56) Zhang, C. Y.; Wang, B.; Wan, Q.; Kong, L.; Zheng, W. L.; Li, Z. C.; Li, L., Critical role of metal ions in surface engineering toward brightly luminescent and stable cesium lead bromide perovskite quantum dots. *Nanoscale* **2019,** *11* (6), 2602-2607.

(57) Zhong, Q.; Cao, M.; Xu, Y.; Li, P.; Zhang, Y.; Hu, H.; Yang, D.; Xu, Y.; Wang, L.; Li, Y.; et al., L-type ligand-assisted acid-free synthesis of $CsPbBr_3$ nanocrystals with near-unity photoluminescence quantum yield and high stability. *Nano Lett.* **2019,** *19* (6), 4151-4157.

(58) Dutta, A.; Dutta, S. K.; Das Adhikari, S.; Pradhan, N., Phase-Stable $CsPbI_3$ Nanocrystals: The Reaction Temperature Matters. *Angew. Chem. Int. Ed.* **2018,** *57* (29), 9083-9087.

(59) Zheng, X.; Yuan, S.; Liu, J.; Yin, J.; Yuan, F.; Shen, W.-S.; Yao, K.; Wei, M.; Zhou, C.; Song, K.; et al., Chlorine Vacancy Passivation in Mixed Halide Perovskite Quantum Dots by Organic Pseudohalides Enables Efficient Rec. 2020 Blue Light-Emitting Diodes. *ACS Energy Lett.* **2020,** *5* (3), 793-798.

(60) Zhang, B.-B.; Yuan, S.; Ma, J.-P.; Zhou, Y.; Hou, J.; Chen, X.; Zheng, W.; Shen, H.; Wang, X.-C.; Sun, B.; et al., General mild reaction creates highly luminescent organic-ligand-lacking halide perovskite nanocrystals for efficient light-emitting diodes. *J. Am. Chem. Soc.* **2019,** *141* (38), 15423-15432.

(61) Kumar, S.; Jagielski, J.; Yakunin, S.; Rice, P.; Chiu, Y.-C.; Wang, M.; Nedelcu, G.; Kim, Y.; Lin, S.; Santos, E. J.; et al., Efficient blue electroluminescence using quantum-confined two-dimensional perovskites. *ACS Nano* **2016,** *10* (10), 9720-9729.

(62) Wu, Y.; Wei, C.; Li, X.; Li, Y.; Qiu, S.; Shen, W.; Cai, B.; Sun, Z.; Yang, D.; Deng, Z.; et al., In situ passivation of $PbBr_6^{4-}$ octahedra toward blue luminescent $CsPbBr_3$ nanoplatelets with near 100% absolute quantum yield. *ACS Energy Lett.* **2018,** *3* (9), 2030-2037.

(63) Hoye, R. L.; Lai, M.-L.; Anaya, M.; Tong, Y.; Gałkowski, K.; Doherty, T.; Li, W.; Huq, T. N.; Mackowski, S.; Polavarapu, L.; et al., Identifying and reducing interfacial losses to enhance color-pure electroluminescence in blue-emitting perovskite nanoplatelet light-emitting diodes. *ACS Energy Lett.* **2019,** *4* (5), 1181-1188.

(64) Yuan, S.; Wang, Z. K.; Xiao, L. X.; Zhang, C. F.; Yang, S. Y.; Chen, B. B.; Ge, H. T.; Tian, Q. S.; Jin, Y.; Liao, L. S., Optimization of Low-Dimensional Components of Quasi-2D Perovskite Films for Deep-Blue Light-Emitting Diodes. *Adv. Mater.* **2019,** *31* (44), 1904319.

(65) Xing, J.; Zhao, Y.; Askerka, M.; Quan, L. N.; Gong, X.; Zhao, W.; Zhao, J.; Tan, H.; Long, G.; Gao, L.; et al., Color-stable highly luminescent sky-blue perovskite light-emitting diodes. *Nat. Commun.* **2018,** *9* (1), 1-8.

(66) Liu, Y.; Cui, J. Y.; Du, K.; Tian, H.; He, Z. F.; Zhou, Q. H.; Yang, Z. L.; Deng, Y. Z.; Chen, D.; Zuo, X. B.; et al., Efficient blue light-emitting diodes based on quantum-confined bromide perovskite nanostructures. *Nat. Photonics* **2019,** *13* (11), 760-764.

(67) Karlsson, M.; Yi, Z.; Reichert, S.; Luo, X.; Lin, W.; Zhang, Z.; Bao, C.; Zhang, R.; Bai, S.; Zheng, G.; et al., Mixed halide perovskites for spectrally stable and high-efficiency blue light-emitting diodes. *Nat. Commun.* **2021,** *12* (1), 361-361.

(68) Jiang, Y.; Qin, C.; Cui, M.; He, T.; Liu, K.; Huang, Y.; Luo, M.; Zhang, L.; Xu, H.; Li, S.; et al., Spectra stable blue perovskite light-emitting diodes. *Nat. Commun.* **2019,** *10* (1), 1-9.

(69) Cheng, L.; Yi, C.; Tong, Y.; Zhu, L.; Kusch, G.; Wang, X.; Wang, X.; Jiang, T.; Zhang, H.; Zhang, J.; et al., Halide Homogenization for High-Performance Blue Perovskite Electrohiminescence. *Research* **2020,** *2020*, 9017871.

(70) Kondo, Y.; Yoshiura, K.; Kitera, S.; Nishi, H.; Oda, S.; Gotoh, H.; Sasada, Y.; Yanai, M.; Hatakeyama, T., Narrowband deep-blue organic light-emitting diode featuring an organoboron-based emitter. *Nat. Photonics* **2019,** *13* (10), 678-682.

(71) Lee, H. L.; Chung, W. J.; Lee, J. Y., Narrowband and Pure Violet Organic Emitter with a Full Width at Half Maximum of 14 nm and y Color Coordinate of Below 0.02. *Small* **2020,** *16* (14), 1907569.

(72) Xue, S.; Qiu, X.; Ying, S.; Lu, Y.; Pan, Y.; Sun, Q.; Gu, C.; Yang, W., Highly Efficient Nondoped Near-Ultraviolet Electroluminescence with an External Quantum Efficiency Greater Than 6.5% Based on a Carbazole-Triazole Hybrid Molecule with High and Balanced Charge Mobility. *Adv. Opt. Mater.* **2017,** *5* (21), 1700747.

(73) Okumoto, K.; Shirota, Y., New class of hole-blocking amorphous molecular materials and their application in blue-violet-emitting fluorescent and green-emitting phosphorescent organic electroluminescent devices. *Chem. Mater.* **2003,** *15* (3), 699-707.

(74) Kwak, J.; Bae, W. K.; Lee, D.; Park, I.; Lim, J.; Park, M.; Cho, H.; Woo, H.; Yoon, D. Y.; Char, K.; et al., Bright and efficient full-color colloidal quantum dot light-emitting diodes using an inverted device structure. *Nano Lett.* **2012,** *12* (5), 2362-2366.

(75) Yang, Y.; Zheng, Y.; Cao, W.; Titov, A.; Hyvonen, J.; Manders, J. R.; Xue, J.; Holloway, P. H.; Qian, L., High-efficiency light-emitting devices based on quantum dots with tailored nanostructures. *Nat. Photonics* **2015,** *9* (4), 259-266.

(76) Wang, L.; Lin, J.; Hu, Y.; Guo, X.; Lv, Y.; Tang, Z.; Zhao, J.; Fan, Y.; Zhang, N.; Wang, Y.; et al., Blue quantum dot light-emitting diodes with high electroluminescent efficiency. *ACS Appl. Mater. Interfaces* **2017,** *9* (44), 38755-38760.

(77) Zhang, H.; Chen, S.; Sun, X. W., Efficient red/green/blue tandem quantum-dot light-emitting diodes with external quantum efficiency exceeding 21%. *ACS Nano* **2018,** *12* (1), 697-704.

(78) Wang, A.; Shen, H.; Zang, S.; Lin, Q.; Wang, H.; Qian, L.; Niu, J.; Li, L. S., Bright, efficient, and color-stable violet ZnSe-based quantum dot light-emitting diodes. *Nanoscale* **2015,** *7* (7), 2951-2959.

(79) Kim, T.; Kim, K.-H.; Kim, S.; Choi, S.-M.; Jang, H.; Seo, H.-K.; Lee, H.; Chung, D.-Y.; Jang, E., Efficient and stable blue quantum dot light-emitting diode. *Nature* **2020,** *586* (7829), 385-389.

(80) Yuan, F.; Yuan, T.; Sui, L.; Wang, Z.; Xi, Z.; Li, Y.; Li, X.; Fan, L.; Tan, Z. a.; Chen, A.; et al., Engineering triangular carbon quantum dots with unprecedented narrow bandwidth emission for multicolored LEDs. *Nat. Commun.* **2018,** *9* (1), 1-11.

(81) Zhang, X.; Zhang, Y.; Wang, Y.; Kalytchuk, S.; Kershaw, S. V.; Wang, Y.; Wang, P.; Zhang, T.; Zhao, Y.; Zhang, H.; et al., Color-switchable electroluminescence of carbon dot light-emitting diodes. *ACS Nano* **2013,** *7* (12), 11234-11241.

(82) Li, Y.; Yin, W.; Deng, R.; Chen, R.; Chen, J.; Yan, Q.; Yao, B.; Sun, H.; Wei, S.-H.; Wu, T., Realizing a SnO_2-based ultraviolet light-emitting diode via breaking the dipole-forbidden rule. *NPG Asia Mater.* **2012,** *4* (11), e30.

(83) Qian, F.; Gradecak, S.; Li, Y.; Wen, C.-Y.; Lieber, C. M., Core/multishell nanowire heterostructures as multicolor, high-efficiency light-emitting diodes. *Nano Lett.* **2005,** *5* (11), 2287-2291.